Active Human Body Model Predictions Compared to Volunteer Response in Experiments with Braking, Lane Change, and Combined Manoeuvres

Emma Larsson, Johan Iraeus, Jason Fice, Bengt Pipkorn, Lotta Jakobsson, Erik Brynskog, Karin Brolin, Johan Davidsson

Abstract Active human body models are an important tool to study occupant interaction with safety systems in evasive manoeuvres such as braking and/or steering. In this study a finite element human body model with and without closed-loop active muscle control in the neck and lower trunk was compared to volunteer occupants in six different load cases with lane change, braking, and combined manoeuvres using standard and pre-pretensioned seat belts. Seven different muscle controllers, using two different muscle activation strategies based either on head and torso displacements or muscle length, and one with the controller turned off have been compared to volunteer kinematics. Cross-correlation analysis with CORA was used to evaluate the model biofidelity. The results show an improvement in CORA scores when using active muscles, compared to the model with muscle activity turned off, for one load case and similar CORA scores between the models for five load cases. CORA scores ranged from 0.78 to 0.88 for the active models and 0.70 to 0.82 from the model with muscles turned off. The active model gave a kinematic response with good biofidelity in lane change with braking, pure braking, and lane change with pre-pretensioned seat belt, but the biofidelity of the model was rated as fair in lane change with standard seat belt.

Keywords Active muscle, closed-loop feedback control, human body model, pre-crash/pre-impact manoeuvre.

I. INTRODUCTION

Many car crashes are preceded by a manoeuvre such as braking and/or steering [1], either by the driver, or automatic crash avoidance systems. During these evasive manoeuvres, the occupant will be exposed to accelerations which could influence the occupant position and response in the possible subsequent crash phase [2-3]. Human body models (HBMs) fitted with active muscular control are an important tool to study occupant interaction with safety systems in these evasive manoeuvres. These computational models have been historically limited to the crash phase and have recently been fitted with active muscle control systems [4-5]. The models are designed as such to replicate human responses in selected evasive manoeuvres and/or subsequent crash scenarios. The evasive manoeuvres are characterised by low-level loading and long duration, whilst the crash phase consist of higher loads and shorter durations [6].

Models available today utilise two different strategies to transition the simulation from an evasive manoeuvre to a crash phase. One strategy uses the same HBM for both phases, which gives the option of running both the evasive manoeuvre and crash phase in one single simulation [2][5][7]. The other uses separate models for the separate phases and maps the state of the model from the final state of evasive manoeuvre to initial position for in-crash [8]. There are models that can handle braking scenarios [5][9], and models that handle scenarios with lateral accelerations [10].

The SAFER HBM v9, representing an averaged sized male, has the capacity to predict the occupant response in both the evasive manoeuvre and the crash in a single simulation. To date the model has been validated in several types of braking events [5][11]. Recently an omni-directional control strategy for neck and lower trunk musculature was designed for the THUMS v3.0, with the intention that the strategy would be implemented into the SAFER HBM model and thereafter compared to data from volunteer experiments [12]. Currently, the implemented coordinate system referencing for SAFER HBM active muscle controllers does not accurately

E. Larsson (e-mail: emma.larsson@chalmers.se; tel: +46-31-7723647) and E. Brynskog are PhD students, J. Iraeus and J. Fice are Researchers, K. Brolin is a Professor and J. Davidsson is an Associate Professor at the Department of Mechanics and Maritime Sciences at Chalmers University of Technology, Gothenburg, Sweden. B. Pipkorn is Director of Simulation and Active Structures at Autoliv Research, Vårgårda, Sweden. L. Jakobsson is a Senior Technical Leader in Injury Prevention at Volvo Cars, Sweden. B. Pipkorn and L. Jakobsson are Adjunct Professors at Chalmers University of Technology, Sweden.

simulate an occupant not aligned in global X axes or load cases with large vehicle rotations.

There are several available volunteer experiments representative of evasive manoeuvre loading that include males in low-level, long duration scenarios. There are several including longitudinal acceleration that simulate braking events, for the driver [13-14] and for the passenger [15-18]. Less including lateral accelerations; for the passengers [19-21]. Experiments [13][16-18][20] were performed with some type of sled system while [14][15][21] were performed with vehicles travelling in real traffic or on a test track. Some of these studies estimated muscle activity by recording electromyography (EMG) [14-16][22], where [14][15][22] reported EMG data normalised to isometric maximum voluntary contraction (MVC) and [16] reported EMG normalised to maximum EMG recorded in all events.

The objective of this study was to extend the capability of SAFER HBM v9 with active muscle control to handle load cases with large vehicle yaw rotations and unaligned positioning in the global coordinate system, and to evaluate the kinematic biofidelity of the HBM compared to the HBM without muscle activation in pure braking, lane change with braking and lane change.

II. METHODS

The SAFER HBM v9 whole body HBM, representing an average-sized male, was used in all simulations. This model is based on the Total HUman Model for Safety AM50 version 3.0 (THUMS; Toyota Motor Corporation 2008). Details about the model used are included in Appendix A. In summary, the model anthropometry was based on the 50th percentile male reported by [23], with a stature of 175cm and weight of 77kg. The model consisted of approximately 127,000 solid elements, 108,000 shell elements, and 2,500 one-dimensional elements. The elements in the model were predominantly hexahedral/quadrilateral and deformable, except for the rigid thoracic vertebrae, sacrum, and vertebral endplates. The musculature in the model were 1D Hill-type elements with activation determined by closed-loop control, as described below. All simulations were performed with the finite element solver LS-DYNA MPP R9.3.0 (LSTC, Livermore, CA, US). Pre- and postprocessing was done with LS-PREPOST (LSTC, Livermore, CA, US) and MATLAB (The Mathworks Inc., Natick, MA, US).

Muscle Activation Control Strategies

Muscle activity was implemented using omni-directional reflex muscle recruitment models consisting of closed loop control with two feedback loops, angular position feedback (APF) and muscle length feedback (MLF), illustrated in Fig. 1 and described in detail in [12]. In short, muscle activities in both the neck and trunk regions were controlled using Proportional-Integral-Derivative (PID) controllers as proposed by [12] (Appendix B, Table IV). Neural delay and muscle activation dynamics was included (Fig. 1 and Appendix B, Table IV). Muscle activation dynamics, from excitation signal ($u=u_{APF}+u_{MLF}$) to activation level (N_a) were modelled as a set of two first order differential equations as described by Winters and Stark [24] (Appendix B, Equations (1) and (2)) and with parameters adapted from [12]. To stabilize joints, a minimum activation level of each muscle was defined based on EMG recorded for passengers during quite sitting in a moving vehicle [12][15] (Appendix B, Table IV).

The neck APF controller emulates vestibular feedback from the central nervous system [12], which reacts to rotations and translations of the head. This reflex aims at stabilising the head in space [25]. The MLF controllers emulate the stretch reflex in the muscles, which in humans are known to contract muscle fibres in response to stretching of muscle spindles [12][25]. Although the omni-directional reflex muscle recruitment models aimed at representing the kinematic response created by human reflexes, it does not attempt to model the central nervous system. Hence, low complexity was chosen for modelling convenience, to enable application of the model in simulations of both evasive manoeuvres and crash, rather than implementing a detailed analogue of the human sensorimotor systems.

The APF controllers implemented in the neck and lower trunk uses two PID controllers, based on omni-directional link angular deviation from reference position, determined at reference time specific for each simulation (Fig. 1), gains proposed by [12] (Appendix B, Table IV). One PID regulates a neck link, defined between the T1 vertebral body and head centre of gravity, and one regulates a lumbar link, defined from the 1st sacral vertebral body to T10 vertebral body. The PID-controllers determine the general target activation level, which is then scaled for each muscle using experimentally derived spatial tuning patterns. During the simulation, scaling muscle activity by spatial tuning patterns is determined by projecting the neck and lumbar links onto the spatial tuning plane [12]. For muscles where experimental spatial tuning patterns were not available, the muscles were

assigned to an available tuning pattern based on similarities in anatomical function [12].

The MLF controllers implemented consisted of multiple PID-controllers, one for each muscle element, based on the elements´ absolute length change from reference length and lengthening velocity. Many muscles were modelled with multiple elements, please see [5] for full details. The MLF controllers activated when the muscle absolute length was above the reference length, determined at the reference time for each simulation. All PID-controllers in the MLF strategy used the same PID controller gains, proposed by [12] (Appendix B, Table IV).

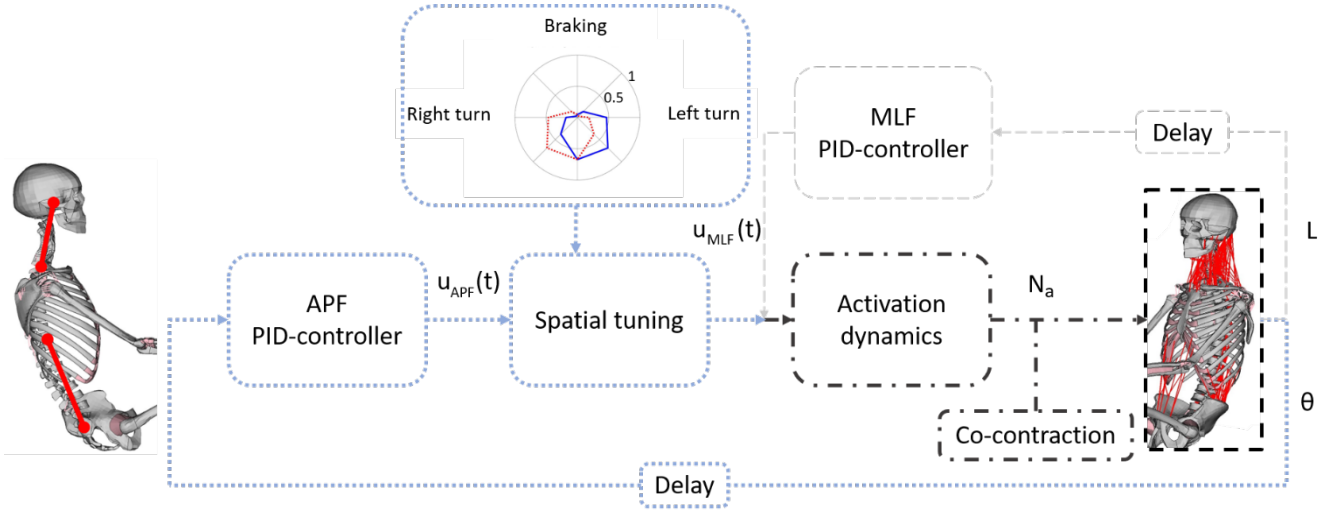

Fig. 1. Illustration of the omni-directional muscle recruitment strategies. Blue dotted lines show APF control loop, where θ is the angle deviation from the reference position of the neck and lumbar links (red lines in left image), in the global coordinate system for the original APF implementation and in the local coordinate systems for the modified APF implementations. $u_{APF}(t)$ is the response from the APF PID controller. Spatial tuning patterns for left (blue) and right (dotted red) sternocleidomastoid is shown as example, where outer grey circle is maximum activation level (1), centre is no muscle activation (0). Grey dashed line shows the MLF control loop, where L is the current absolute length of the muscle element. $u_{MLF}(t)$ is the response from the MLF PID controller. The black dash-dotted parts are common for both loops. Activation dynamics is described in Appendix B.

The original APF implementation, where link angles and spatial tuning scaling were determined in the global coordinate system, was modified to allow for simulations where the HBM sagittal plane was not aligned with the global X-axis (Fig. 2), for example when the vehicle rotates in yaw during a lane change manoeuvre. In this study, three different reference coordinate systems for the APF link angles and spatial tuning have been implemented and the responses compared to those of volunteers. Before pre-positioning, all three-coordinate systems were initially aligned with the global system (Fig. 2). The three reference coordinate systems were: 1) vehicle fixed coordinate system, hereafter called APF-V, where the coordinate system rotates with the vehicle in all axes; 2) partially HBM fixed coordinate system, referred to as APF-Y, where the coordinate system rotated in the yaw direction only based on a vector that connected the T1 and sternum for the neck, and with the sacrum for the lower trunk controller; 3) fully HBM fixed coordinate system, hereafter referred to as APF-L, where the coordinate system rotated with the T1/sternum and sacrum in all three axes. The coordinate systems determined the reference posture that the APF controller attempted to maintain for the body region controlled. The coordinate systems also determined in which plane the spatial tuning was projected. For APF-V it was projected onto the vehicle XY-plane, for APF-Y it was projected onto the global XY-plane (horizontal plane) and for APF-L it was projected onto the T1/sternum and sacrum local XY-planes.

Pre-positioning

A positioning simulation was initially performed to place the HBM in the seat (Fig. 2). This positioning was common for all load cases. The duration of the positioning simulation was 750 ms, divided into two steps. In the first step of the positioning simulation (0-250 ms), gravity loading was applied with muscle controllers turned off. In this step, the head and T1 were translated closer to equilibrium position by prescribing a displacement (8 mm rearward). This was done to prevent large oscillations from subsequent muscle activation. In the second step (250-750ms) muscle activation was added to the gravity load, either using APFs, MLFs or a combination of these.

Reference time, the time when assigning reference positions or reference muscle lengths for the controllers, were set to 250 ms for all controllers with the exception when MLF simulations were combined with APF. Then the MLF reference time was 400 ms to let the APF controllers find a stable position before activating the MLF controllers. All load cases used the same models of the seat and restraint system. The seat model was provided by Volvo Car Company and the compressional quasi-static properties of the seat cushion have previously been validated against a seat identical to those installed in the vehicles used in the volunteer tests [5].

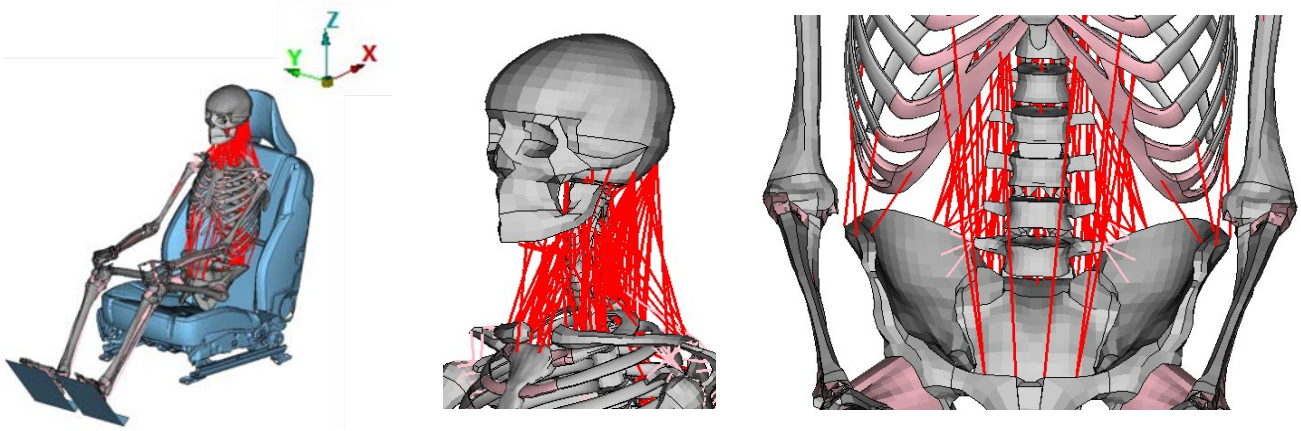

a) HBM positioned in the seat. b) Neck muscle elements c) Lower trunk muscle elements

Fig. 2. The HBM positioned in the seat. Soft tissue and seat belt model are removed for visibility but included in simulations. Muscles controlled by the PID systems are shown in red. Global coordinate system is shown in the top right corner.

Test Setups and Evaluation Data

Two sets of volunteer experiments have been selected for model evaluations. Both these sets include kinematics and muscle activation normalised with MVC for vehicle passengers. One experiment was included to compare model response in lateral and frontal oblique accelerations in form of lane change with and without braking on a test track [19]. The lane changes consisted of two phases: first a right turn and then a left turn. Only the first face was used for the model evaluations. In this experiment a commercially available Volvo V60 model year (MY) 2016 with leather seats was used. The test series contained four scenarios, autonomous lane change with and without braking, performed by a driving robot, with two belt configurations: standard and pre-pretensioned seat belt. The pre-pretensioner applied a target force of 170 N and was activated 200 ms prior to manoeuvre initiation. The electrical reversable pre-pretensioner represented a restraint system in autonomous vehicles, which tensions the belt before the vehicle makes an emergency manoeuvre to avoid a collision. The data set included nine male volunteers with an average (± standard deviation (std)) height and weight of 183 ± 6.1 cm and 72.3 ± 7.7 kg. In the test series, head translations, head rotations, torso translations and seat belt forces were recorded. Muscle activity was recorded and normalised using MVC in 19 muscles of the arms, legs, torso, and neck. Seven of these muscles, Sternocleidomastoid (SCM), Middle Scalene (MS), Upper Trapezius (UTRP), Cervical Paravertebrals (experiment)/ Semispinalis Capitis (HBM) (CPVM), Rectus Abdominis (RA), External Oblique (EXOB), Erector Spinae (longissimus) (LPVM), were included in the active neck and lumbar muscle controller of the HBM and used further in this study.

Another experiment was included in this study for evaluation of the model in longitudinal accelerations in form of autonomous braking on public roads [15]. The full test duration was used for comparison. The volunteer experiment was run in a Volvo V60 MY 2012 with leather seats, with two belt configurations: standard and pre-pretensioned. The pre-pretensioner applied a nominal tension force of 170 N and was activated 200 ms prior to manoeuvre initiation. The data set included 11 male volunteers with an average (± std) height and weight of 178.2 ± 5.2 cm and 77.5 ± 5.6 kg. The study recorded head translations and rotations, sternum and T1 translations, seat belt and foot well forces. Muscle activity was recorded and normalised using MVC in eight muscles, of which four were included and activated in the HBM's active neck and lumbar muscle controllers; SCM, CPVM, LPVM and RA.

All six load cases were run using APF-Y, APF-Y+MLF, and passive controllers (Table I). The APF-Y controller (with and without MLF) was evaluated in all load cases because it was believed to replicate the vestibulocollic reflex the most, since the controller always has a global vertical reference. To evaluate the difference between the different APF implementations, one load case (lane change with braking, standard seat belt) has been run with

all implemented muscle recruitment strategies (Table I). This load case was chosen because it includes both braking and steering, letting the occupant move away from the back support and at the same time moving out of the seat belt. In all simulations averaged pulses from the volunteer experiment were applied (Fig. 3). In the autonomous braking cases, separate accelerations were reported for the experiments with standard seat belt and pre-pretensioned seat belts. In the simulations the average vehicle acceleration from the experiments with pre-pretensioned belt was used also for the simulations with standard seat belt.

In the lane change load cases, t0 was defined as manoeuvre initiation. For the lane change load case simulations, with and without braking, including pre-pretensioner the retractor was started 280 ms before the event t0 (after a simulation time of 470 ms) and ramped to target force during 450 ms. For the pure braking cases, t0 was defined as when vehicle acceleration reached 5% of the peak value (approximately 0.3 s, shown with the leftmost dashed vertical line in Fig. 3c). For the pure braking load case simulations with pre-pretensioner, the retractor was started 257 ms before the event t0 (after a simulation time of 640 ms) and ramped to target force during 450 ms.

TABLE I
SIMULATIONS CARRIED OUT IN THIS STUDY

	Lane change with and without braking [19]				Pure braking [15]	
	No braking, standard seatbelt	No braking, pre-pretensioned seatbelt	Braking, standard seatbelt	Braking, pre-pretensioned seatbelt	Standard seatbelt	Pre-pretensioned seatbelt
APF-L			X			
APF-V			X			
APF-Y	X	X	X	X	X	X
APF-L+MLF			X			
APF-V+MLF			X			
APF-Y+MLF	X	X	X	X	X	X
MLF			X			
Passive	X	X	X	X	X	X

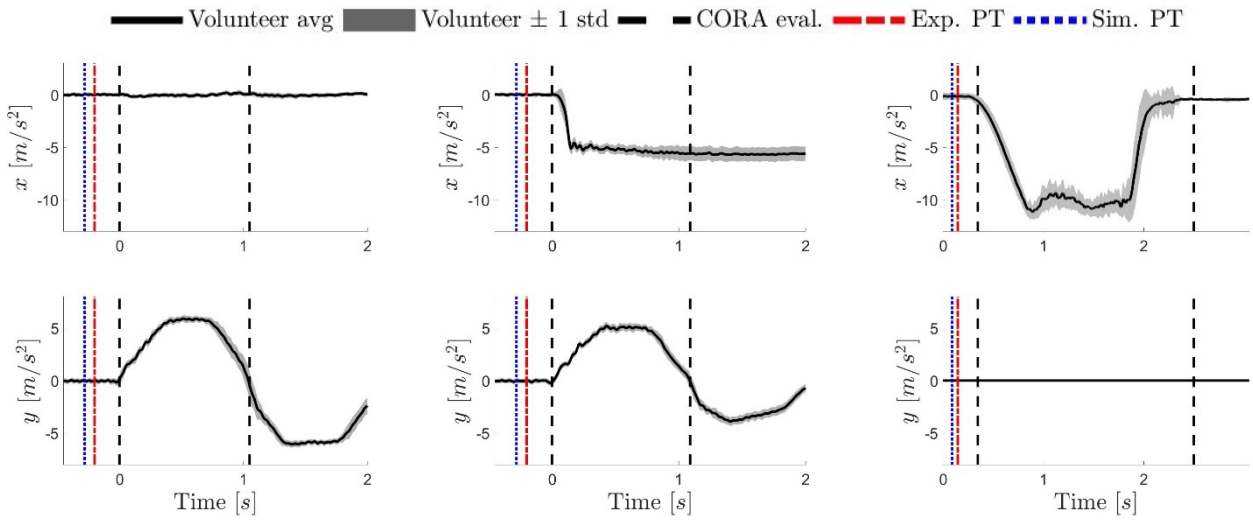

a) Lane change without braking b) Lane change with braking c) Pure braking

Fig. 3. Average acceleration pulses [m/s^2] in longitudinal (x, top) and lateral (y, bottom) from the volunteer experiments. Average acceleration in black and ±1 standard deviation in grey [15][19]. For pure braking cases, no lateral (Y) acceleration was reported, an assumption of zero lateral acceleration was made for the simulations. Black dotted lines show evaluation interval, left dotted line shows event t0 at 0s for both lane change cases and approximately 0.3s for pure braking. Timing for activation of seatbelt pre-pretensioner is shown as red dash-dotted (volunteer experiments) and blue dotted (simulations) lines.

Data analysis

To evaluate the biofidelity of the SAFER HBM v9 with active muscle control systems, kinematic response and muscle activation time histories have been compared to the volunteer data. The comparisons were done by plotting experimental results together with simulation results, as well as by evaluation of correlation using the CORAplus 4.0.4 software [26]. Different weights have been used for the evaluation of kinematics (and forces) and for the evaluation of muscle activation (Table II). Kinematics and forces were evaluated using the proposed settings in the CORAplus software manual [27], using average volunteer response as reference, inner corridor as ±1 standard deviation and outer corridor as ±2 standard deviations [28]. The model active muscle controller outputs were evaluated by calculating the cross-correlation CORA score between the model and each volunteer's EMG response and then a subject wise average and standard deviation of these cross-correlation scores were presented. This was done because of variability in timing and shape for the EMG recordings, meant that the mean response may not be a meaningful representation of the data, rendering the corridor approach invalid. The phase-shift evaluations were removed for the muscle activation evaluation because it was seen that in the case of no activation at all, the phase shift gave a perfect correlation. For the muscles consisting of more than one muscle element, with a controller using MLF where each element has an individual activation signal, each element activation signal was compared to the individual volunteer EMG recordings. Average and standard deviation was calculated using all CORA scores for that muscle, i.e. a muscle consisting of three elements, in a case where 24 EMG recordings were collected from the volunteer experiments, the average was calculated using 72 CORA scores. To facilitate easier interpretation the CORA ratings were categorised as *excellent*, *good*, *fair* and *poor* in accordance with [27] (Table II). A relevant difference in CORA scores was defined as 0.14, as this is the difference between the "good" and "excellent" CORA score thresholds [27]. For muscle activity, a relevant difference was defined as a difference in average of above 0.14, and no overlap in standard deviation range.

TABLE II
CORA SETTINGS

		Kinematics/forces	**Muscle activity**
Weights	Corridor rating	0.5	0.0
	Cross-correlation rating	0.5	1.0
	Shape	0.5	0.66
	Size	0.25	0.33
	Phase-shift	0.25	0.0
Limits on CORA rating	Excellent	>0.94	
	Good	>0.80	
	Fair	>0.58	
	Poor	<=0.58	

For lane change (with and without braking) the CORA evaluation was performed from event t0 (start of manoeuvre, 0s) until the lateral vehicle acceleration had changed direction (approximately 1 s), which represents the first turn in the lane change cases. The reason to exclude the second turn was that from viewing experimental videos it was apparent that some volunteers did not attempt to maintain an upright posture during the second turn, suggesting the influence of voluntary control and the HBM muscle controllers currently only simulate reflexive responses. For the pure braking cases, t0 was defined as when vehicle acceleration reached 5% of the peak value (approximately 0.3 s, shown with the leftmost dashed vertical line in Fig. 3). The CORA evaluation was performed fromt0 until end of simulation (approximately 2.5 s).

To create an overall CORA score for each model, the model CORA scores were summed using a weighting procedure; the measures were grouped in three groups; body translations, body rotations and belt forces. Within the three groups, the weighting factors for each measure was based on the peak magnitude of that measure divided by the maximum peak value within the group, so the measures with the largest peak magnitudes in each group contributed the most to the group rating. The groups were summed using the number of measures in the group, i.e., translations in lane change account for 55% of the overall rating, since there were six measured translations (3 axes for head and torso) and 11 measures in total. Muscle activity was not included in the overall rating since muscle activity is not available for the passive model.

All kinematic results were presented in the vehicle coordinate system according to [29] (Z-Down), with X positive axis in forward vehicle direction, positive Y axis from left to right in the vehicle and positive Z direction

downwards. For the lane change (with and without braking) load cases, the changes in rotation of the head were calculated using extrinsic Euler angles $Z_1Y_2X_3$, as described in the volunteer study [19]. In the pure braking cases, the rotations were calculated as the angle change between Frankfort plane and horizontal plane (XY-plane) in the XZ-plane [15].

III. RESULTS

Lane Change with Braking

The head kinematics in the first phase (between black dashed lines in Fig. 3, Fig. 4) in simulated lane change with braking and standard seat belt, models with APF-Y and APF-Y+MLF muscle controllers provided rather similar displacements and rotational displacements as did the average volunteer, whilst the passive model provided larger displacements. (Fig. 4). T1 translational kinematics in X and Y were similar between all three simulation models and volunteers, and all three models produced higher lap belt forces compared to volunteers (Appendix C, Fig. 11).

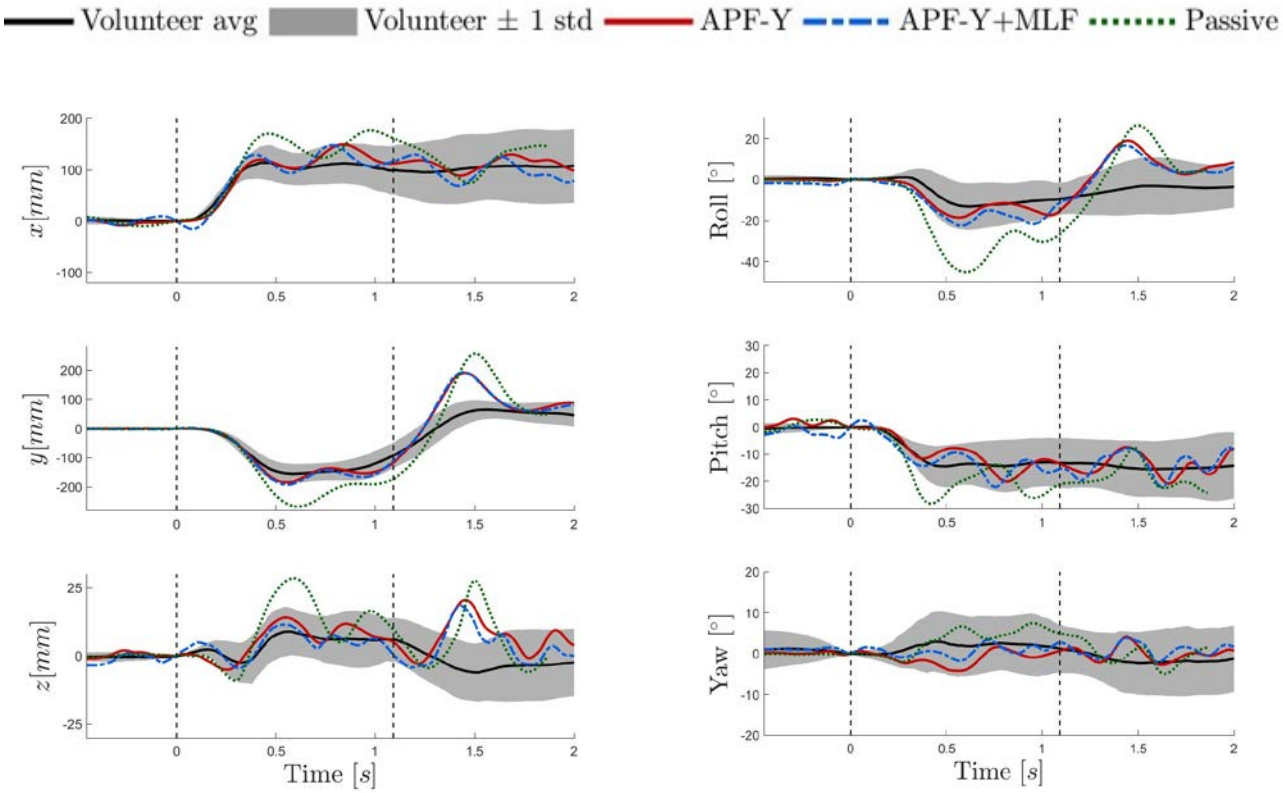

a) Translational kinematics *[mm]* b) Rotational kinematics *[°]*

Fig. 4. Head kinematics for lane change with braking, standard seatbelt. Grey curves show average ± 1 std for volunteers [19], red curves show APF-Y HBM response, blue dashed show APF-Y+MLF response and dotted green curves show passive HBM response. Black dotted lines show evaluation interval.

When comparing CORA scores of kinematic responses and forces for APF-Y, APF-Y+MLF and passive models it was seen that head Y displacement and roll provided higher CORA scores for the active models compared to the passive model, while the passive model provided higher CORA scores than the active models for head yaw (Fig. 5). The APF-Y model provided higher CORA scores compared to the passive model for shoulder belt force and head x displacement, while the passive model provided a higher CORA score in T1 Z displacement. The APF-Y+MLF model provided higher CORA scores compared to the passive model in head Z displacement and compared to the APF-Y model in T1 Z displacement (Fig. 5).

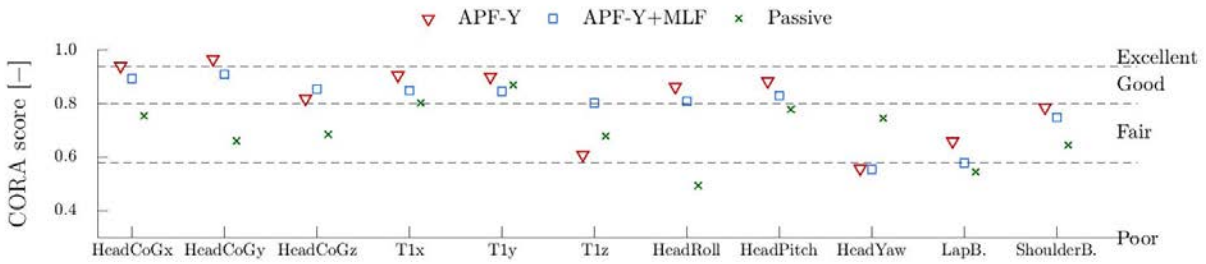

Fig. 5. CORA scores [-] for lane change with braking, standard seat belt for APF-Y (red), APF-Y+MLF (blue) and passive (green) models respectively.

It appears that models with active musculature (APF-Y & APF-Y+MLF) exhibited gross motions in closer agreement to that of an exemplar volunteer than the model with passive musculature did (Fig. 6). The volunteer shows less head roll relative to the vehicle than all three model configurations at 0.5 s, possibly aiming at keeping his head aligned with gravity.

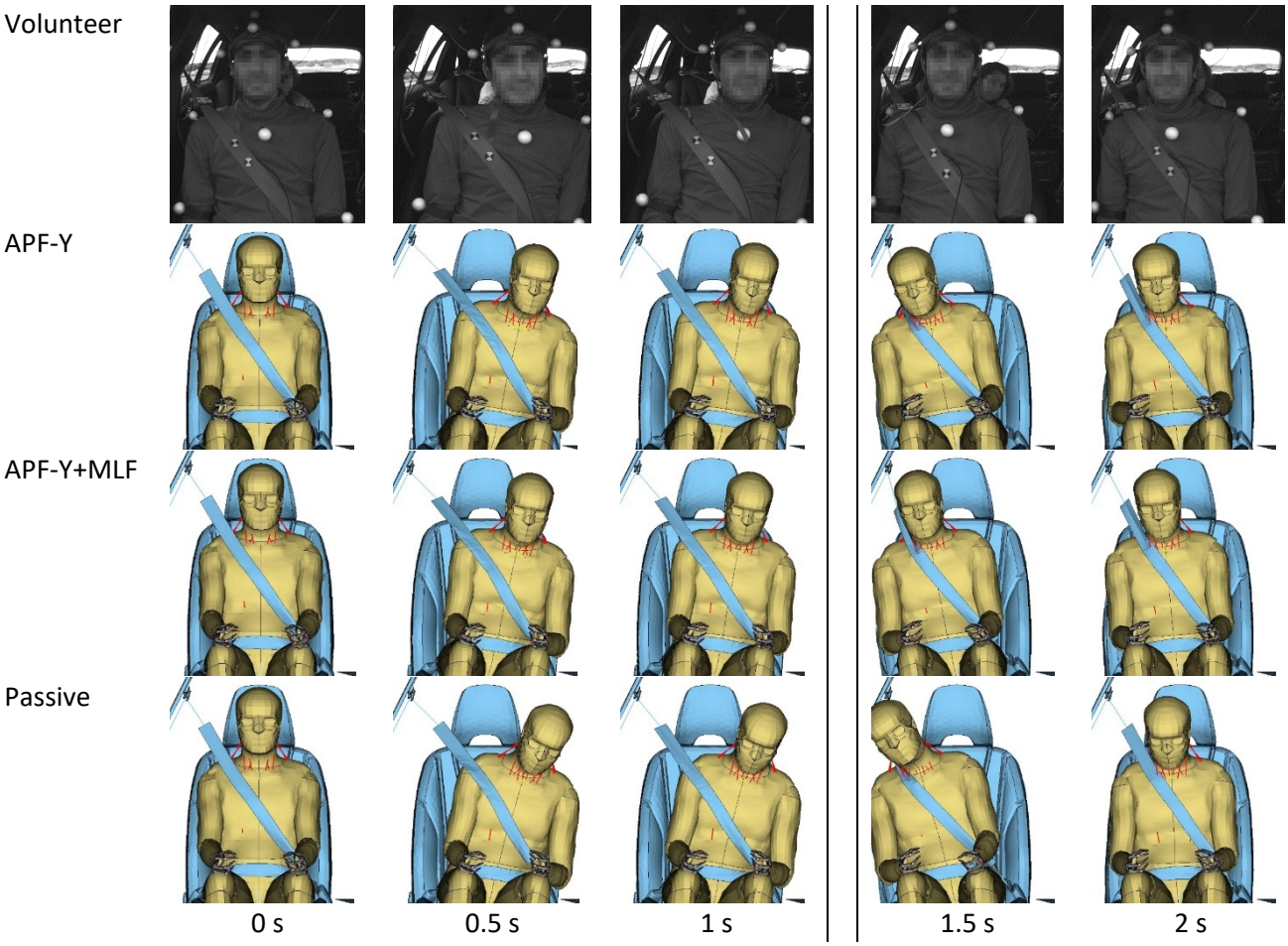

Fig. 6. Snapshots of one volunteer compared to HBM in lane change with braking, with the vertical lines representing end of evaluation using the CORA method.

In the comparison of average CORA ratings for muscle activation between APF-Y and APF-Y+MLF the APF-Y+MLF gave similar results, except for SCM and MS where APF-Y+MLF gave lower CORA scores. All muscles correlated poorly to the volunteer EMG (Fig. 7). APF-Y+MLF gave bursts of muscle activation not seen in only APF-Y configuration for SCM, CPVM, RA, MS and UTRP (Appendix C, Fig. 12). EXOB and LPVM showed similar activity between APF-Y and APF-Y+MLF configurations (Appendix C, Fig. 12), which was reflected in the similarity in CORA averages and standard deviations (Fig. 7).

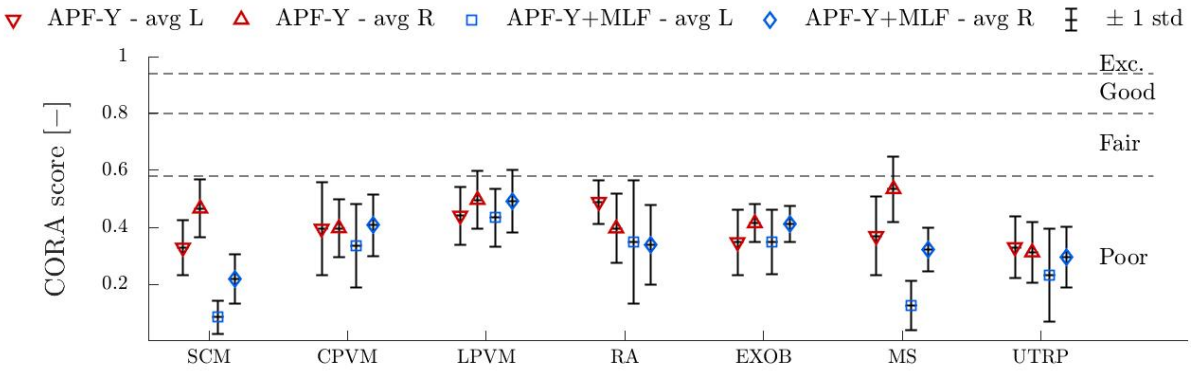

Fig. 7. Average muscle activation CORA rating [-] (average and standard deviation) in lane change with braking, standard seat belt using APF-Y and APF-Y+MLF. As previously presented, the scores were calculated by comparing the output of the active muscle controller to each volunteer's EMG response using the CORA cross-correlation score and then presenting the subject wise average and standard deviation.

Lane Change without Braking

In lane change without braking, standard seat belt, head y translations of simulation models were similar to the volunteer average response, while the head yaw was opposite in direction between simulation models and volunteer average (Appendix C, Fig. 13). T1 Y translation was similar but slightly lower in the simulations compared to volunteers, and peak lap belt force was higher in simulations compared to in experiments (Appendix C, Fig. 14).

CORA scores show excellent correlation between all three model results and volunteer average in head Y translation, and good correlation in T1 Y translation and shoulder belt forces. Relevant difference between simulation models is found in T1 Z translation where the passive model shows higher correlation compared to both active models, and in head roll, where both active models show higher correlation compared to the passive model (Fig. 8).

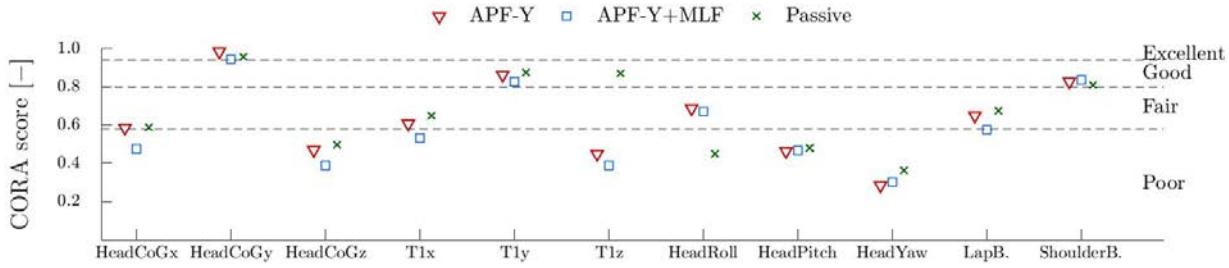

Fig. 8. CORA scores [-] for lane change without braking, standard seat belt for APF-Y (red), APF-Y+MLF (blue) and passive (green) models respectively.

Pure Braking

Simulations of the load case braking with pre-pretensioned seat belt provided similar head and T1 displacements compared to those of the volunteers for all tested muscle control systems (APF-Y, APF-Y+MLF and passive). The only exception was for sternum Z-displacements which were lower and opposite in direction than volunteer displacements for all models. The head Y-rotations for the two active models were closer to the average volunteer response compared to that of the passive model. The two active models showed oscillations in head Z translations and head rotations, induced by the control system (Fig. 9).

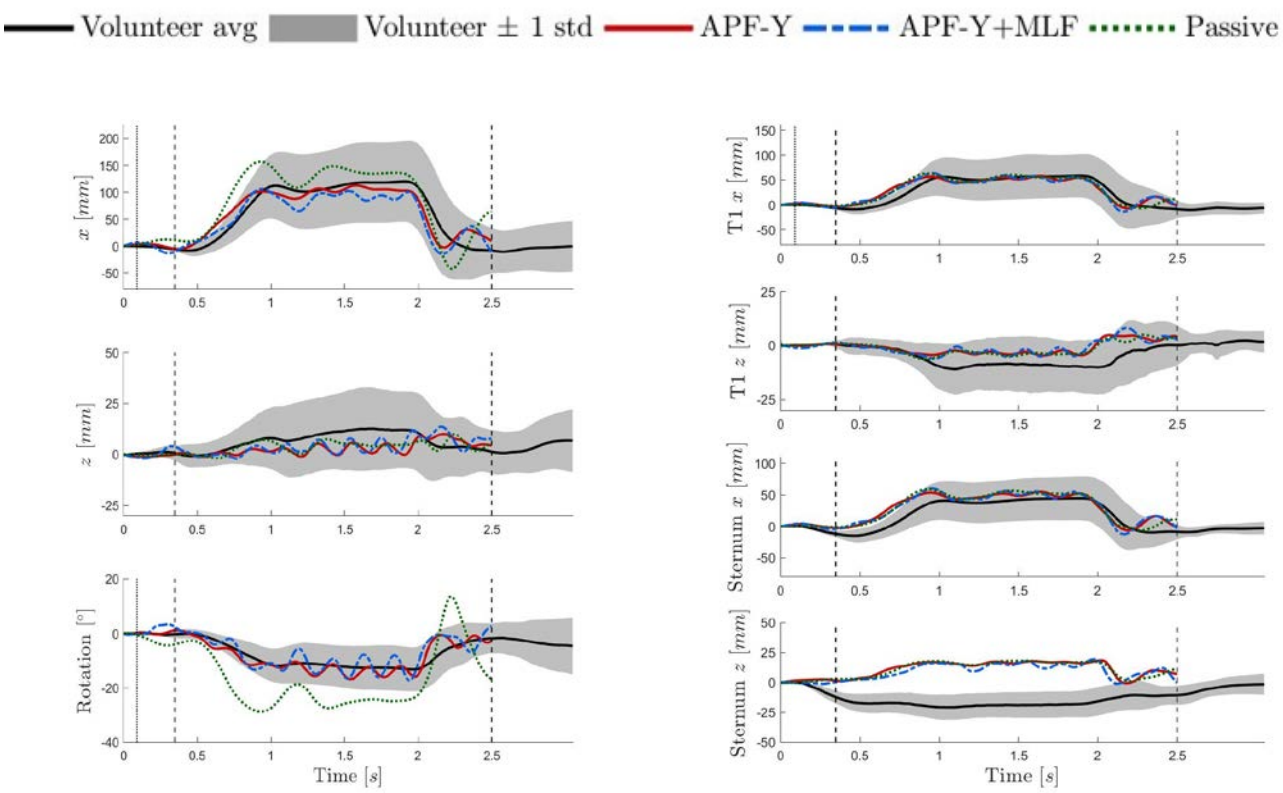

a) Head kinematics b) Torso kinematics

Fig. 9. Kinematics for braking with pre-pretensioned seatbelt. Grey curves show average ± 1 std for volunteers [15], red curves show APF-Y HBM response, blue dashed shows APF-Y+MLF response and dotted green curves show passive HBM response.

CORA rankings for the different measures indicate that all three models correlate similarly to the volunteers, and no relevant differences were found between any of the models in any of the measures (Fig. 10)

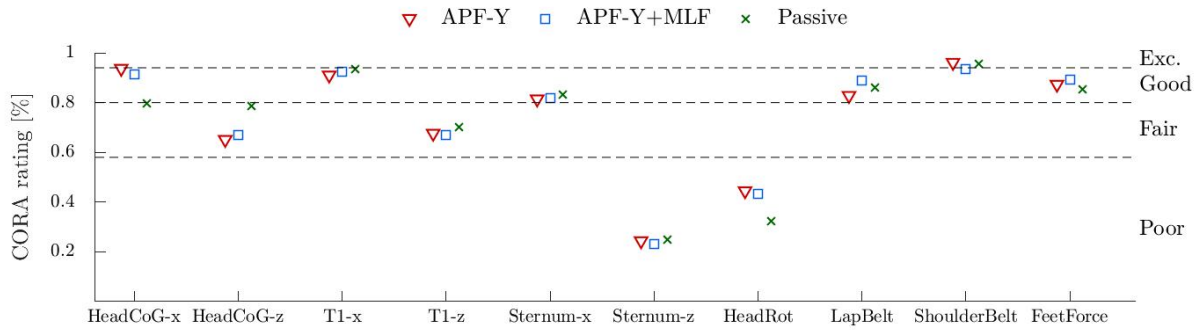

Fig. 10. CORA scores for pure braking, pre-pretensioned seat belt with APF-Y, APF-Y+MLF and passive control strategy.

CORA comparison

When comparing the overall CORA scores for simulations of all six load cases the models provided similar CORA scores between active models and passive model. In lane change with braking and standard seatbelt a relevant difference was found, where the APF-V and APF-Y models gave a higher correlation compared to the passive and APF-L+MLF models. For the other five load cases a trend of improvement in CORA scores for active models was observed, but the increase was smaller and potentially not as relevant. No relevant differences were found when comparing scores for the six different load cases, where maximum difference for APF-Y was 0.10 (lane change without braking, standard seatbelt compared to lane change with braking, pre-pretensioned seatbelt), for APF-Y+MLF it was 0.09 (lane change without braking, standard seatbelt compared to pre-pretensioned seatbelt), and

for passive 0.12 (lane change with braking, standard seatbelt compared to pre-pretensioned seatbelt), (Table III).

TABLE III
OVERALL CORA SCORE FOR ALL SIMULATIONS

	Lane change with and without braking [19]				Pure braking [15]	
	No braking, standard seatbelt	No braking, pre-pretensioned seatbelt	Braking, standard seatbelt	Braking, pre-pretensioned seatbelt	Standard seatbelt	Pre-pretensioned seatbelt
APF-L			0.75			
APF-V			0.87			
APF-Y	0.78	0.84	0.86	0.88	0.81	0.82
APF-L+MLF			0.71			
APF-V+MLF			0.82			
APF-Y+MLF	0.74	0.83	0.82	0.82	0.80	0.81
MLF			0.81			
Passive	0.74	0.80	0.70	0.82	0.77	0.78

IV. DISCUSSION

The objective of the study was to evaluate the biofidelity of the active SAFER HBM v9 using different omnidirectional muscle recruitment strategies compared to the same HBM without muscle activation in lane change, lane change with braking and pure braking. The study showed that the HBM with active muscles using APF-Y and APF-V gave better correlation to the volunteer tests than the same model in passive configuration in lane change with braking, standard seat belt, while in the other five load cases no relevant difference was observed (Table II). There were small differences between the different control strategies, where the only relevant difference was found between APF-V/APF-Y and APF-L+MLF during lane change with standard seat belt.

Muscle Activation Control Strategies

For this paper the emphasis has been on the APF-Y strategy. APF-Y was included for all load cases, whereas APF-V and APF-L were compared in selected load cases. The original APF strategy in the neck link, before the modifications from this study, was designed to return the head to a vertical alignment relative to a global reference [12], which was introduced to mimic the vestibulocollic reflex. This similarity to the vestibulocollic reflex was maintained in APF-Y, because the reference angle was always relative to a global vertical. In the other control strategies, if the vehicle (APF-V) or the torso (APF-L) have rotated in pitch or roll then the posture the controller seeks to maintain may not be aligned with the global vertical axis. The volunteers tendency of maintaining the initial vertical head alignment (in the gravity field) is seen in the photo comparison (Fig. 6). This is something that is lacking in APF-L and MLF and to some extent also in APF-V. Therefore, the APF-Y was chosen as the best candidate for the study. However, this might not be the best selection if using the HBM in a reclined position or during a roll-over event, where head link angles would be projected onto the spatial tuning patterns in the horizontal plane and lead to biomechanically unsuitable muscle activity. In that case, the spatial tuning might need to follow the occupant, as in APF-L, while reference angle is kept connected to gravity.

Similarly, the APF-V implementation would likely not be able to handle reclined occupants either, again since head-link angles would be projected onto another plane. The spatial tuning in APF-V would most likely work better than APF-Y in a roll-over, where the HBM rotates with the vehicle. However, in roll-over the alignment of local Z-axis in gravity field would be lost.

Another issue with spatial tuning for reclined passengers or in roll-over is that the curves were collected in the horizontal plane for a standard seated posture. If the model capabilities should be extended to include these cases or vertical loading, additional data will be needed.

The CORA scores comparing the APF muscle controllers' output to volunteer EMG were generally classified as poor. There are potential issues when comparing the muscle controller output with EMG signals. The main issue when comparing volunteer EMG traces to the muscle controller output was that the muscle controller is not an analogue for the complete human sensorimotor system and thus it may be unreasonable to expect the two to

produce the identical output. A further issue is that comparing our muscle controller to EMG is that the activation signal used in the muscle elements is a filtered version of the PID signal and more resembles the force output from a muscle. Whilst the EMG measures the interference pattern of signals propagating along the muscle fibres and approximates the neural drive going to the muscle and not the force output. In the simulation model, there is no signal that directly corresponds to what is measured with the EMG, although according to [30], it could be comparable to the PID signal that is fed to the activation dynamics (u). However, in the active HBM model co-contraction was added to the muscle activation signal after the activation dynamics, if the activity suggested by the controller was below the co-contraction level. Therefore, to include the co-contraction for size comparison in the CORA evaluation, the filtered signal (N_a) was used in the CORA evaluation.

When comparing LHS and RHS for lane change simulations where MLF is included, it was seen that for some load cases and muscles there was a difference between CORA scores for left-hand side (LHS) and right-hand side (RHS) muscles. The APF implementations also show a CORA score bilateral asymmetry, but not to the same extent. One example is the MS using APF-Y+MLF where the RHS muscle gives a better CORA score compared to the LHS muscle (Fig. 7). This better correlation was also seen when visually comparing time histories of the MS muscle activation to volunteer EMG traces, where both volunteers and models had two peaks of activity in the RHS MS during the second half of the evaluation interval, although some difference in timing is seen between volunteers and HBM muscle activation (Fig. 12).

Kinematics

In the lane change without braking simulations, the head yaw rotations showed a difference in behaviour between model and volunteer response (Fig. 13). While the HBM followed the response expected considering the inertial loading applied, the volunteer trend was the opposite. This might be an effect of volitional control, or the vestibulocollic reflex opposing the head yaw induced by the vehicle manoeuvre. The same limitation from rotational control was seen in the comparison between model results and volunteer in lane change with braking and standard seat belt, where the model showed larger head roll than the exemplar volunteer (Fig. 6), and in the time history plots of rotational kinematics in the same load case, where the models showed larger roll rotations compared to the volunteer average, but within the standard deviation (Fig. 4). Since the control system controls neck-link angle rather than head rotations directly and the controller represents reflexive and not volitional control, our results in this study showed that this behaviour cannot be captured accurately. Furthermore, in a post-hoc analysis on the APF-Y controller during the braking plus lane change without pre-pretensioner, we showed that CORA scores decreased (max change of -0.07) as the evaluation period increased from 1.3 to 1.6 s after manoeuvre onset. This decrease in CORA score may be related to a lack of representation of volitional control, which may grow in influence as the manoeuvre unfolds.

In lane change with braking and standard seatbelt, when comparing the CORA scores for kinematic measures (Fig. 5) and the visual match of the model behaviour to one exemplar volunteer (Fig. 6), it may be argued that the CORA scores seem higher than may be expected. Although this is only a qualitative visual analysis. The model visually showed a larger head roll compared to the exemplar volunteer, but the roll kinematic response was within the corridor for both active models, perhaps due to variably between subjects, and the time histories of roll showed a visual similarity in shape, which led to good and excellent scores in corridor and cross correlation ratings (Fig. 4). The corridor rating constituted 50% and cross correlation 25% of the CORA score, leading to a total CORA score rated as good for both active models. The passive model CORA score for roll was rated as poor.

In the lane change manoeuvre without braking, the torso (T1 & sternum) in the passive model translates laterally less than the volunteers (Fig. 14), and when muscle activity is added the model's translation is further reduced. The volunteer EMG data suggested that volunteers were using muscle activity to limit their lateral translation (Fig. 15) and it is therefore expected that a passive model should translate laterally more than volunteers in a lane change load case. The reduced translation of the passive model compared to volunteers suggests that the passive stiffness of the torso is too high in the lateral direction.

Limitations

No calibration of the controller gains has been performed and it is known that reflexive gains in humans are context dependant, not fixed [31]. The APF gains are taken from a sagittal plane controller which has been calibrated to a set of volunteer braking data and validated to another set [11]. Some improvement in correlation would be expected if the gains were calibrated for the implemented controllers using representative loading. The

MLF gains have not been calibrated, and all PID-controllers in MLF used the same gains. Improvements could be expected if the gains were calibrated, either still using the same gains for all controllers, or using some grouping, or individually for each muscle element controller.

To reduce the number of simulations no combinations of coordinate system configurations have been run. Neck and lower trunk have used the same controller configuration, and with the same coordinate system for spatial tuning angle as for the PID reference vector. Another option could be to use APF-Y for the reference position to keep alignment with gravity but use APF-L for the spatial tuning.

For both lane change and pure braking load cases the evaluation period was long enough to include volitional movement, and this is a limitation for our implementation of muscle control which only captures reflexive behaviour. For the upper limb the volitional epoch from a disturbance is considered to be as early as 100ms, reviewed in [32]. In the experimental load cases considered in the study, head motion of the volunteers begins at approximately 150-200 ms after manoeuvre onset. A rough approximation would be that the subjects could voluntarily react to the manoeuvres by approximately 250-300 ms, which means a large portion of the model evaluation intervals may have included voluntary responses from the subjects we are trying to simulate. The design of muscle controllers that can generate reflexive and volitional responses is important future work.

V. CONCLUSIONS

This study compared kinematic responses and seat belt forces predicted by the active SAFER HBM v9 using different omnidirectional muscle recruitment strategies compared to the same HBM without muscle activation and volunteers in braking, lane change, and combined manoeuvres. The study shows that the HBM with active muscles using a control strategy with a coordinate system that remained aligned with gravity gave a better correlation to the volunteer tests than the same model in a passive configuration for lane change with braking and standard seat belt. Similar patterns, but with smaller and potentially less relevant changes, were found between active and passive models for lane change without braking, pure braking and lane change with braking and pre-pretensioned belt. It is concluded that the HBM with active musculature gave a kinematic response with good biofidelity in lane change with braking, pure braking, and lane change with pre-pretensioned seat belt, but the biofidelity of the model was rated as fair in lane change with standard seat belt.

VI. ACKNOWLEDGEMENT

The authors would like to acknowledge Jóna Marin Olafsdottir for the APF and MLF controllers. The work was carried out at SAFER – Vehicle and Traffic Safety Centre at Chalmers, Gothenburg, Sweden. It was funded by FFI (Strategic Vehicle Research and Innovation), by VINNOVA, the Swedish Transport Administration, the Swedish Energy Agency and the industrial partners. The project partners are Chalmers, Volvo Cars, Autoliv Development and Dynamore Nordic AB in Sweden. Simulations were performed on resources at Chalmers Centre for Computational Science and Engineering (C3SE) provided by the Swedish National Infrastructure for Computing (SNIC).

VII. REFERENCES

[1] Talmor, D., Legedza, A.T.R., and Nirula, R. Injury thresholds after motor vehicle crash—Important factors for patient triage and vehicle design. *Accident Analysis & Prevention*, 2010. 42(2): p. 672-675

[2] Bose, D., Crandall, J.R., Untaroiu, C.D., and Maslen, E.H. Influence of pre-collision occupant parameters on injury outcome in a frontal collision. *Accident Analysis & Prevention*, 2010. 42(4): p. 1398-1407

[3] Hault-Dubrulle, A., Robache, F., Drazétic, P., and Morvan, H. Pre-crash phase analysis using a driving simulator. Influence of atypical position on injuries and airbag adaptation. *Proceedings of Proc. of the 21st ESV Conf*, 2009.

[4] Fice, J.B., Cronin, D.S., and Panzer, M.B. Cervical Spine Model to Predict Capsular Ligament Response in Rear Impact. *Annals of Biomedical Engineering*, 2011. 39(8): p. 2152-2162

[5] Östh, J., Brolin, K., Carlsson, S., Wismans, J., and Davidsson, J. The Occupant Response to Autonomous Braking: A Modeling Approach That Accounts for Active Musculature. *Traffic Inj. Prev.*, 2012. 13(3): p. 265-277

[6] Osth, J., Olafsdóttir, J.M., Davidsson, J., and Brolin, K. Driver kinematic and muscle responses in braking events with standard and reversible pre-tensioned restraints: validation data for human models. *Stapp Car Crash J*, 2013. 57: p. 1-41

[7] Daichi Kato, Yuko Nakahira, Noritoshi Atsumi, and Masami Iwamoto Development of Human-Body Model THUMS Version 6
containing Muscle Controllers and Application to Injury Analysis in Frontal Collision after Brake Deceleration *Proceedings of IRCOBI*, 2018. Athens (Greece)
[8] Katsunori Yamada,
Mitsuaki G., Yuichi Kitagawa, Tsuyoshi Yasuki Simulation of Occupant Posture Change during Autonomous E mergency Braking and Occupant Kinematics in Frontal Collision. *Proceedings of IRCOBI*, 2016. Malaga (Spain)
[9] Iwamoto, M., Nakahira, Y., Kimpara, H., Sugiyama, T., and Min, K. Development of a Human Body Finite Element Model with Multiple Muscles and their Controller for Estimating Occupant Motions and Impact Responses in Frontal Crash Situations. *SAE Technical Papers*, 2012. 2012-October(October)
[10] Iwamoto, M. and Nakahira, Y. Development and Validation of the Total HUman Model for Safety (THUMS) Version 5 Containing Multiple 1D Muscles for Estimating Occupant Motions with Muscle Activation during Side Impacts. *SAE Technical Papers*, 2015(November)
[11] Östh, J., Brolin, K., and Bråse, D. A Human Body Model With Active Muscles for Simulation of Pretensioned Restraints in Autonomous Braking Interventions. *Traffic Inj. Prev.*, 2015. 16(3): p. 304-313
[12] Ólafsdóttir, J.M., Östh, J., Brolin, K. Modelling Reflex Recruitment of Neck Muscles in a Finite Element Human Body Model for Simulating Omnidirectional Head Kinematics. *Proceedings of IRCOBI*, 2019. Florence (Italy)
[13] Kemper, A.R., Beeman, S.M., Madigan, M.L., and Duma, S.M. Human Occupants in Low-Speed Frontal Sled Tests: Effects of Pre-Impact Bracing on Chest Compression, Reaction Forces, and Subject Acceleration. *Traffic Inj. Prev.*, 2014. 15: p. S141-S150
[14] Östh, J., Ólafsdóttir, J.M., Davidsson, J., and Brolin, K. Driver Kinematic and Muscle Responses in Braking Events with Standard and Reversible Pre-tensioned Restraints: Validation Data for Human Models. *SAE Techni. Paper.*, 2013. 2013-November(November)
[15] Ólafsdóttir, J.M., Östh, J.K.H., Davidsson, J., and Brolin, K.B. Passenger kinematics and muscle responses in autonomous braking events with standard and reversible pre-tensioned restraints. *Proceedings of IRCOBI*, 2013. Gothenburg (Sweden)
[16] Ejima, S., Ono, K., Holcombe, S., Kaneoka, K., and Fukushima, M. A study on occupant kinematics behaviour and muscle activities during pre-impact braking based on volunteer tests. *Proceedings of IRCOBI*, 2007.
[17] Dehner, C., Schick, S., et al. Muscle activity influence on the kinematics of the cervical spine in frontal tests. *Traffic Inj Prev*, 2013. 14(6): p. 607-13
[18] Daisuke Ito, Susumu Ejima, et al.
Occupant Kinematic Behavior and Effects of a Motorized Seatbelt on Occupant Restraint of Human Volunte ers during Low Speed Frontal Impact: Mini-sled Tests with Mass Production Car Seat. *Proceedings of IRCOBI*, 2013. Gothenburg (Sweden)
[19] Ghaffari, G., Brolin, K., et al.
Passenger kinematics in Lane change and Lane change with Braking Manoeuvres using two belt configurations: standard and reversible pre-pretensioner *Proceedings of IRCOBI*, 2018. Athens (Greece)
[20] Arbogast, K.B., Mathews, E.A., et al. The effect of pretensioning and age on torso rollout in restrained human volunteers in far-side lateral and oblique loading. *Stapp Car Crash J*, 2012. 56: p. 443-467
[21] Huber, P., Kirschbichler, S., Prüggler, A., and Steidl, T. Passenger kinematics in braking, lane change and oblique driving maneuvers. *Proceedings of IRCOBI*, 2015.
[22] Ghaffari, G., Brolin, K., Pipkorn, B., Jakobsson, L., and Davidsson, J. Passenger Muscle Responses in Lane Change and Lane Change with Braking Manoeuvres using two belt configurations: standard and reversible pre-pretensioner. *Traffic Injury Prevention, in press*, 2019
[23] Robbins, D. Anthropometric specifications for mid-sized male dummy. *US Department of Transportation DTNH22-80-C-07502, Washington, DC*, 1983. 2
[24] Winters, J.M. and Stark, L. Analysis of fundamental human movement patterns through the use of in-depth antagonistic muscle models. *IEEE transactions on biomedical engineering*, 1985(10): p. 826-839
[25] Keshner, E.A. Vestibulocollic and cervicocollic control. *Encyclopedia of neuroscience*, 2009: p. 4220-4224
[26] Gehre, C., Gades, H., and Wernicke, P. Objective Rating of Signals Using Test and Simulation Responses. *Proceedings: International Technical Conference on the Enhanced Safety of Vehicles*, 2009. 2009
[27] Thunert, C. CORAplus Release 4.0.4 User's Manual. 2017.

[28] Östh, J., Mendoza-Vazquez, M., Linder, A., Svensson, M.Y., and Brolin, K. The VIVA OpenHBM finite element 50th percentile female occupant model: Whole body model development and kinematic validation. *Proceedings* 2017.
[29] Vehicle Dynamics Terminology. 2008, SAE International.
[30] Winters, J.M. and Stark, L. Analysis of Fundamental Human Movement Patterns Through the Use of In-Depth Antagonistic Muscle Models. *IEEE Transactions on Biomedical Engineering*, 1985. BME-32(10): p. 826-839
[31] Forbes, P.A., Dakin, C.J., et al. Frequency response of vestibular reflexes in neck, back and lower limb muscles. *American Journal of Physiology-Heart and Circulatory Physiology*, 2013
[32] Kurtzer, I.L. Long-latency reflexes account for limb biomechanics through several supraspinal pathways. *Frontiers in integrative neuroscience*, 2015. 8: p. 99

VIII. APPENDIX

A. Modifications to the THUMS v3 model

Body Part		Modification
Muscles	**Neck and lower trunk**	**Hill-type muscle elements added** "Östh, J., Brolin, K., Carlsson, S., Wismans, J., and Davidsson, J. The Occupant Response to Autonomous Braking: A Modeling Approach That Accounts for Active Musculature. Traffic Inj. Prev., 2012. 13(3): p. 265-277."
	Shoulder	**Hill-type muscle elements added** "Östh, J., Brolin, K., and Bråse, D. A Human Body Model With Active Muscles for Simulation of Pretensioned Restraints in Autonomous Braking Interventions. Traffic Inj. Prev., 2015. 16(3): p. 304-313."
	Legs	**Hill-type muscle elements added** "Östh, J., Eliasson, E., Happee, R., and Brolin, K. A method to model anticipatory postural control in driver braking events. Gait Posture, 2014. 40(4): p. 664-669."
Chest	**Ribs**	**Geometry and mesh modified** "Shi X, Cao L, Reed MP, Rupp JD, Hoff CN, Hu J. (2014) A statistical human rib cage geometry model accounting for variations by age, sex, stature and body mass index. *Journal of biomechanics. 2014;47(10): pp. 2277-2285.*" **Cortical bone thickness modified** "Choi H-Y, Kwak D-S. (2011) Morphologic Characteristics of Korean Elderly Rib. J. Automot. Saf. Energy. 2011;2" **Cortical bone properties modified** "Kemper AR, McNally C, Kennedy EA, *et. al*. (2005) Material properties of human rib cortical bone from dynamic tension coupon testing. *Stapp Car Crash Journal. 2005;49: pp. 199-230.* "Kemper AR, McNally C, Pullins CA, Freeman LJ, Duma SM, Rouhana SM. The biomechanics of human ribs: material and structural properties from dynamic tension and bending tests. *Stapp Car Crash Journal. 2007;51: pp. 235-273*."
	Sternum	**Geometry and mesh modified** 50^{th} percentile male sternum "Weaver, A.A., Schoell, S.L., Nguyen, C.M., Lynch, S.K., Stitzel, J.D. Morphometric analysis of variation in the sternum with sex and age. *Journal of morphology. 2014; 275 (11), pp. 1284-1299.*"
Lumbar Spine	**Vertebra**	**Remeshed** Contact between vertebra and intervertebral disk added Intervertebral ligaments modified – both geometry and properties "Afwerki, H. (2016) Biofidelity Evaluation of Thoracolumbar Spine Model in THUMS. Master's Thesis in Biomedical Engineering, *Chalmers University of Technology, 2016*"
Head		**New Head Model**

"Kleiven, S. (2007). Predictors for Traumatic Brain Injuries Evaluated through Accident Reconstructions. *51st Stapp Car Crash Journal,2007: pp. 81-114.*"

B. Controller Parameters

TABLE IV
CONTROLLER PARAMETERS

Control strategy	Parameter	Value
APF and MLF	*Neck Co-contraction level*	0.05
	Lumbar Co-contraction level	0.03
	Time constant, neural excitation - T_{ne}*	35 ms
	Time constant, muscle activation - $T_{na,a}$*	10 ms
	Time constant, muscle deactivation - $T_{na,d}$*	40 ms
APF	*Neck neural delay*	20 ms
	Neck link – Proportional gain	1.301 1/rad
	Neck link – Integral gain	0 1/rad ms
	Neck link – Derivative gain	470 1/rad ms^{-1}
	Lumbar neural delay	25 ms
	Lumbar link - Proportional gain	1.210 1/rad
	Lumbar link - Integral gain	0 1/rad ms
	Lumbar link - Derivative gain	159 1/rad ms^{-1}
MLF	*Neural delay*	10 ms
	Proportional gain	0.5 1/mm
	Integral gain	0 1/mm ms
	Derivative gain	5 1/mm ms^{-1}

* These constants were used two first order differential equations proposed by Winters and Stark [24], presented in Equations (1) and (2), where u is the muscle controller signal, N_e an intermediate neural excitation level and N_a the excitation signal used in the muscle elements.

$$\frac{dN_e}{dt} = \frac{(u - N_e)}{T_{ne}} \tag{1}$$

$$\frac{dN_a}{dt} = \begin{cases} \frac{(N_e - N_a)}{T_{na,a}}, & N_e \geq N_a \\ \frac{(N_e - N_a)}{T_{na,d}}, & N_e < N_a \end{cases} \tag{2}$$

C. Simulation Results

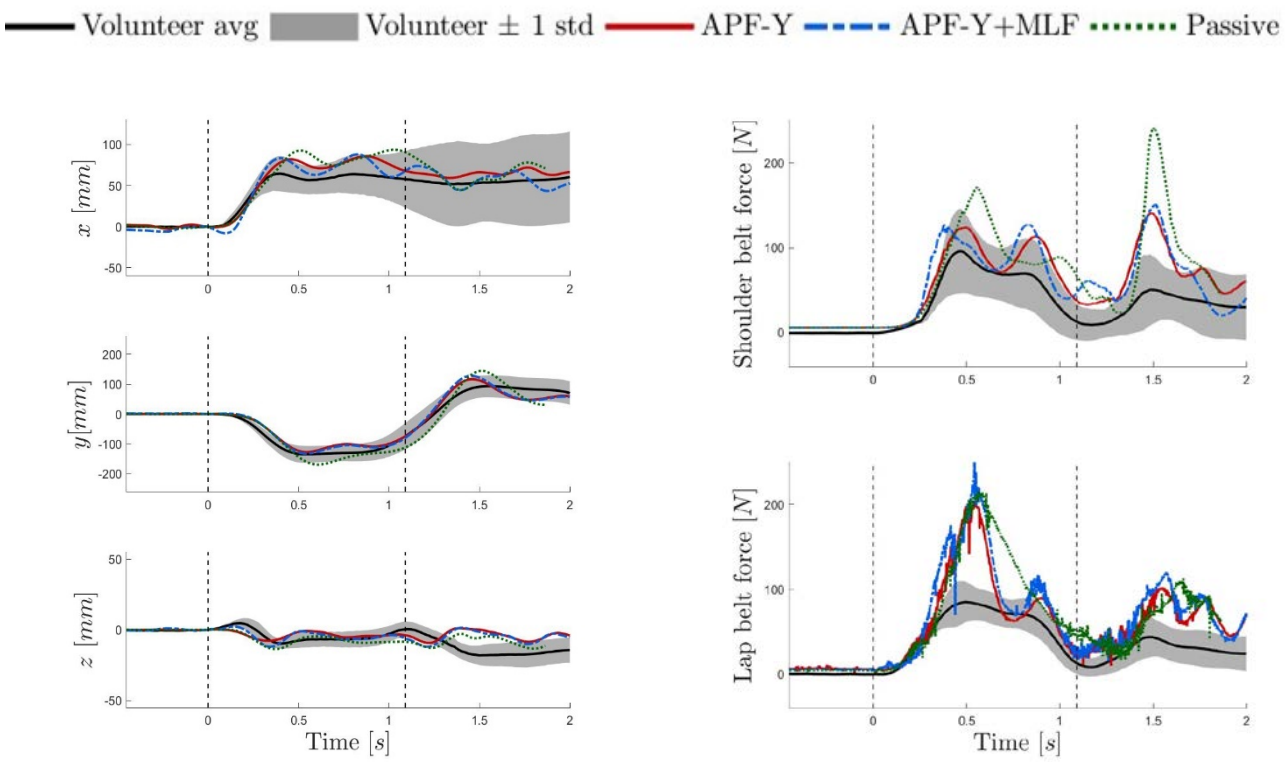

a) T1 translational kinematics b) Seatbelt forces

Fig. 11. T1 translational kinematics and seatbelt forces for lane change with braking, standard seat belt. Grey curves show average ± 1 std for volunteers [19], red curves show APF-Y HBM response, blue dashed shows APF-Y+MLF response and dotted green curves show passive HBM response.

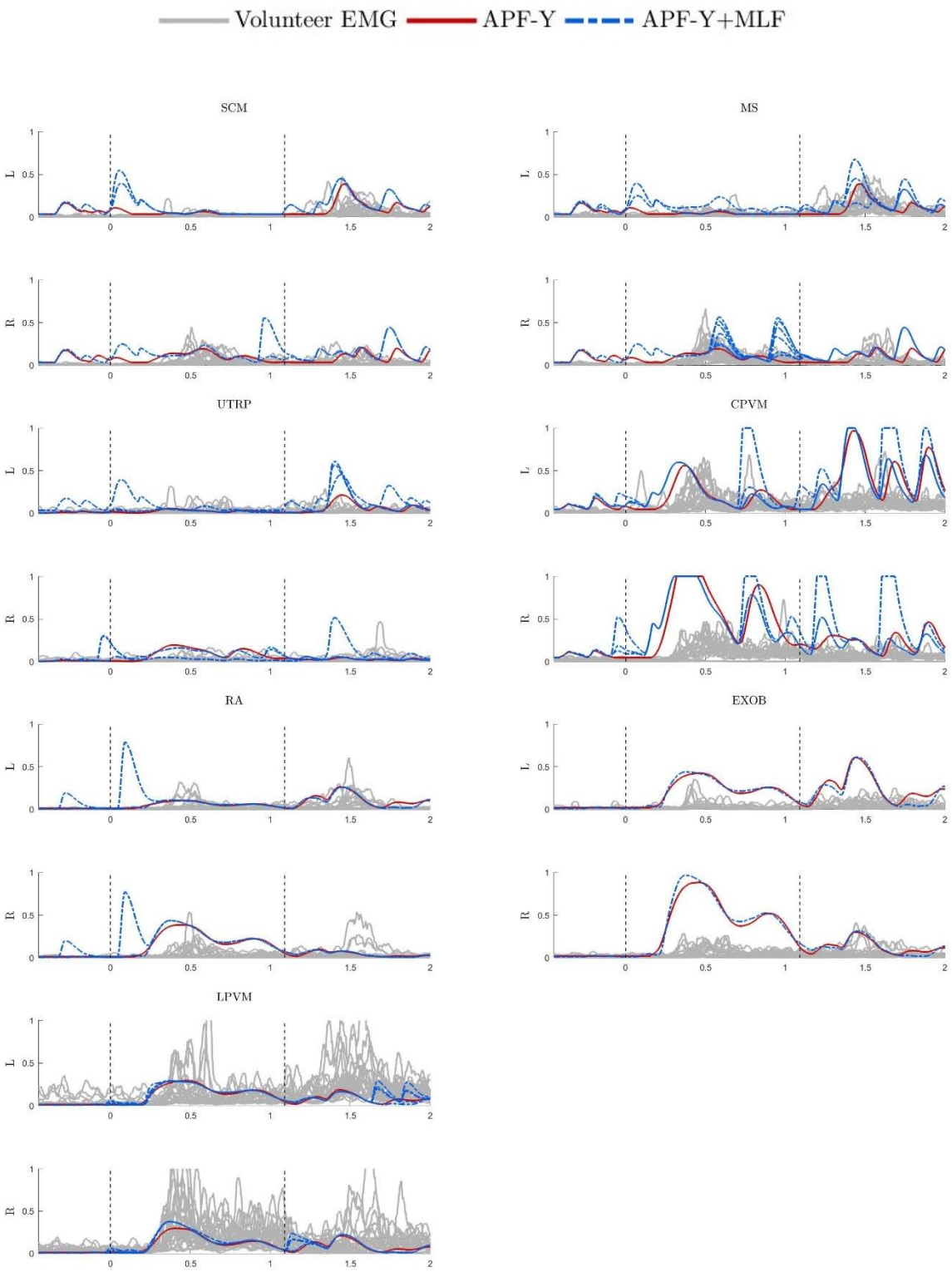

Fig. 12. Muscle activation in lane change with braking, standard seat belt. Grey curves show individual EMG recordings for volunteers normalized using MVC [22], red curves show APF-Y HBM activation and blue dashed show APF-Y+MLF activation. For some muscles there are multiple blue lines, where each blue line represents one muscle element response in the MLF control strategy.

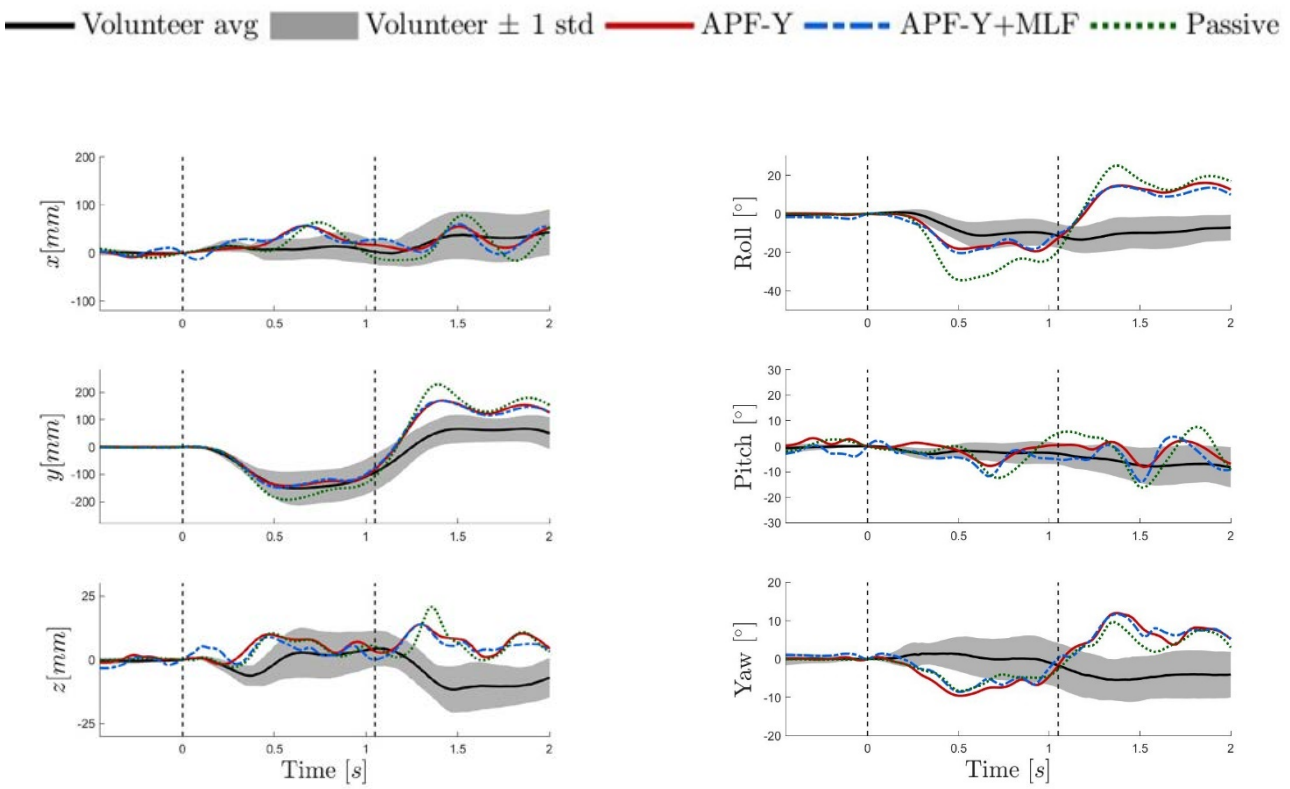

a) Translational kinematics b) Rotational kinematics

Fig. 13. Head kinematics for lane change without braking, standard seat belt. Grey curves show average ± 1 std for volunteers[19], red curves show APF-Y HBM response, blue dashed show APF-Y+MLF response and dotted green curves show passive HBM response.

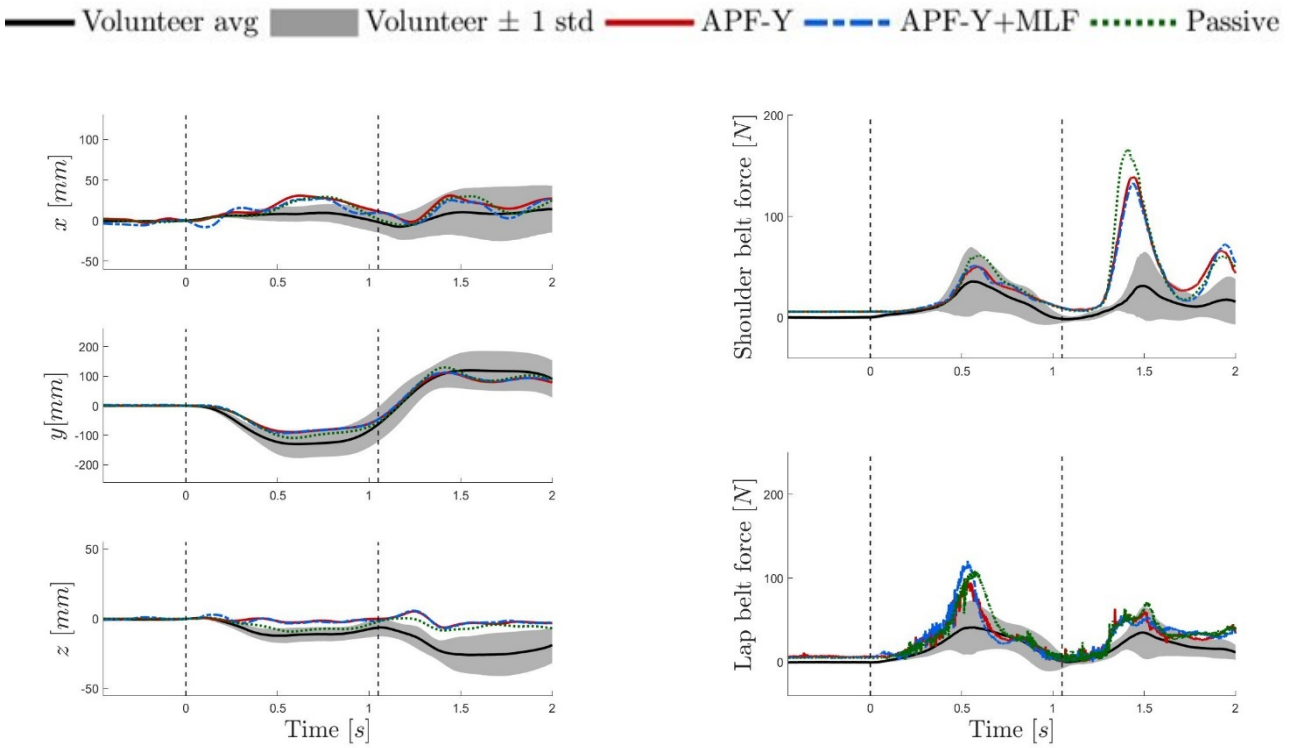

a) T1 translational kinematics *[mm]* b) Seatbelt forces

Fig. 14. T1 translational kinematics for lane change without braking, standard seat belt. Grey curves show average ± 1 std for volunteers [19], red curves show APF-Y HBM response, blue dashed show APF-Y+MLF response and dotted green curves show passive HBM response.

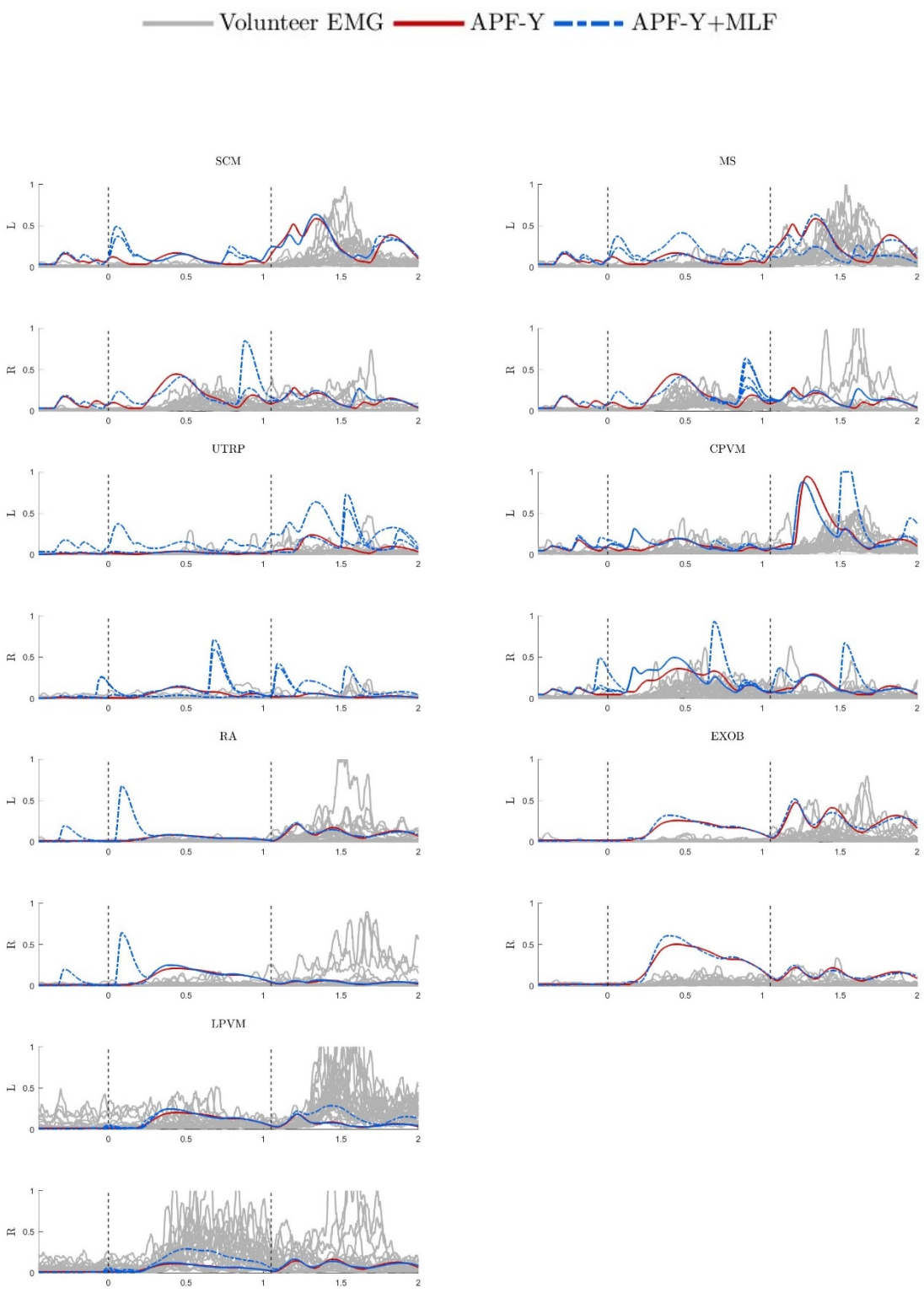

Fig. 15. Muscle activation in lane change with standard seat belt. Grey curves show individual EMG curves for volunteers normalized using MVC [22], red curves show APF-Y HBM activation and blue dashed show APF-Y+MLF activation. For some muscles there are multiple blue lines, where each blue line represents one muscle element response in the MLF control strategy.